Chirality Induction at Helically Twisted Surface of Nanoparticles Generating Circularly Polarized Luminescence

Jumpei Kuno, Nicolas Ledos, Pierre-Antoine Bouit, Tsuyoshi Kawai, Muriel Hissler, Takuya Nakashima

Chirality Induction at Helically Twisted Surface of Nanoparticles Generating Circularly Polarized Luminescence

Jumpei Kuno,[a] Nicolas Ledos,[b] Pierre-Antoine Bouit,[b] Tsuyoshi Kawai,[a] Muriel Hissler,*[b] and Takuya Nakashima*[a,c]*

[a] Division of Materials Science, Graduate School of Science and Technology, Nara Institute of Science and Technology, 8916-5 Takayama, Nara 630-0192, Japan

[b] Univ Rennes, CNRS, ISCR - UMR 6226, F-35000 Rennes, France

[c] Department of Chemistry, Graduate School of Science, Osaka Metropolitan University, 3-3-138 Sugimoto, Sumiyoshi, Osaka 558-8585, Japan

KEYWORDS. circularly polarized luminescence, chirality, hybrid nanoparticles, coordination

ABSTRACT. Circularly polarized luminescence (CPL) can be generated either from fluorescent dyes with chiral structures or from achiral luminophores in chiral environments such as chiral hosts or chiral self-assemblies. Herein, we demonstrate the CPL induction to an achiral fluorophore grafted on an inorganic nanoparticle (NP) with a chiral shape. Nanoparticles

composed of a mercury sulfide (HgS) cinnabar phase with a chiral crystal structure are investigated as a platform on which the achiral molecules self-assemble into a chiral arrangement. Both the crystallographic and morphological chiralities of HgS NPs are independently considered for the induction of a chiral arrangement of achiral dyes. The HgS NPs with an ellipsoidal shape (NEs) are modified with the achiral fluorescent dye, resulting in no CPL emission. The larger HgS NPs with a chiral twisted structure (NTs) are found to give rise to CPL. The sign of CPL signals could be regulated through the modification of the twist direction of the HgS NPs. Chirality is considered to be induced in the arrangement or assembly of achiral fluorescent molecule on the chirally twisted surface of NPs.

INTRODUCTION

Circularly polarized luminescent (CPL) materials have received broad attention due to their potential applications in 3D displays, [1,2] chiroptical materials,[3,4] and optoelectronic devices.[5–10] Extensive studies have been conducted on the development of CPL-active materials based on chiral organic dyes,[11–14] polymers,[15–18] metal complexes,[19-22] and supramolecular assemblies.[23,24] The most common approaches to obtain CPL-active dyes is a combination of a chiral moiety with a luminophore by a covalent bond or the design of intrinsically chiral luminophores.[25] While such chiral organic dyes sometimes require tediously long synthesis procedures, their CPL performance is not always impressive. An alternative approach includes the coassembly of achiral fluorescent materials with chiral molecules and supramolecular assemblies.[17,24,26-30] The optical activity of chiral molecular systems is successfully transferred into non-chiral luminophores through chiral molecular arrangement and/or chiral electronic hybridization. For

example, cyclodextrins can incorporate achiral guest dyes in their hydrophobic cavity to achieve CPL generation.[26–28] Helical chiral supramolecular assemblies were also employed to coassemble with achiral emitting substrates such as dyes,[29-31] quantum dots[32,33] and perovskite nanocrystals,[34] successfully generating CPL with various colors. The chiral supramolecular assemblies could serve as a template for the chiral assembly of achiral dyes.[29-31] The chiral assemblies also incorporate achiral nanomaterials, providing a chiral electronic environment.[32-35] Although chiral organic systems have been well demonstrated as chiral inducers to stimulate CPL activity partnered with achiral organic and inorganic luminophores, the potential of inorganic materials as a chiral template has rarely been explored.[36-43]

Recently, chirality transfer experiments from metal clusters with an intrinsically chiral atomic arrangement to the organic ligands attached to the surface of the core have been demonstrated.[39] Achiral thiolate ligands coordinated to the surface of the chiral cluster adopt a chiral arrangement on their surface, inducing interligand chiral interactions.[39] Huang and co-workers demonstrated that the chirality of the surface of a chiral silver nanohelix generated by a glancing angle deposition technique was transferred to the stereoselective adsorption of a prochiral anthracene derivative leading to stereoselective photodimerization on the surface of the nanohelix.[40] Helical silica scaffolds also served as a platform for a helical arrangement of achiral molecular chromophores and metal ions.[41,42] To our knowledge, the combination of chiral inorganic NP with achiral luminophore to generate CPL active materials has been limited to a recent example employing helical plasmonic nanorods,[43] while dye grafting to the nanoparticle surface has been extensively studied to promote unusual emission properties. The helical plasmonic nanorods served as a nanopolarizer giving a filtering effect on the emission of achiral fluorophore.[43] From a viewpoint of inorganic-to-organic chirality transfer, cinnabar nanoparticles

are promising to address this challenge. Cinnabar (α-HgS), which crystallizes in the chiral trigonal space group of $P3_121$ (or its enantiomorph $P3_221$), is a potential candidate for a chiral inorganic template. Previous works reported the enantioselective synthesis of colloidal α-HgS nanoparticles (NPs) possessing a chiral crystalline lattice but an achiral ellipsoidal morphology.[44,45] Furthermore, Ouyang and co-workers succeeded in the preparation of α-HgS nanostructures with independently controlled chiral crystalline lattice and helically twisted morphology.[46,47] While the chiral ligand in the initial synthesis of seed defines the crystallographic handedness, the one in the latter growth stage determines the handedness in the twist of morphology with the larger length scale. Herein, we report a new CPL-generation system composed of an achiral luminophore **1** incorporating a grafting unit (Figure 1) and α-HgS NPs. Both the crystallographic and morphological chiralities of HgS NPs were independently considered for the induction of chiral arrangement of **1**. The α-HgS nanoellipisoids (NEs) with the achiral shape could not induce CPL of **1**, whereas CPL signals could be observed upon the combination of **1** and NPs with topological chirality (nanotwists, NTs). The sign of CPL was dependent on the handedness of NT morphology regardless of the crystallographic chirality of NTs.

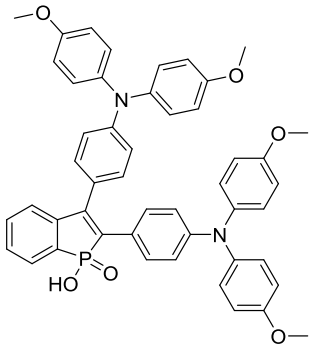

Figure 1. Chemical structure of the achiral fluorophore 1.

EXPERIMENTAL SECTION

General Methods. 1 was synthesized according to the reaction procedures described in the Supporting Information following Scheme S1. Absorption spectra in solution were studied with a JASCO V-760 spectrophotometer. Fluorescence spectra were measured with a spectrofluorometer (Hitachi F7000). Absolute fluorescence quantum yield of **1** was determined by using a Hamamatsu C9920-02. TEM observation was conducted with a JEOL JEM-2200FS electron microscope. Specimens for TEM were prepared by drop-casting of solutions of NEs or NTs onto carbon-coated copper grids. XRD profiles were recorded using a RigakuSmartLab9kW/IP/HY/N X-ray diffractometer. ATR-IR measurements were performed using a JASCO FT/IR-4000 equipped with a JASCO ATR-PRO ONE. CPL spectra were measured using a home-made CPL spectroscopy system.[48]

Synthesis of α-HgS NEs.[44] 39 mg $Hg(NO_3)_2 \cdot nH_2O$ was dissolved in 3.9 ml of water, followed by addition of 0.9 ml of D- or L-penicillamine aqueous solution (100 mM) under stirring to get a colorless solution. An aqueous 100 mM NaOH solution was added to adjust the pH value to *ca.* 11.5. After further stirring for 3 min, 0.9 ml of thioacetamide solution (100 mM) was injected quickly and the mixture was stirred for 24 h at room temperature for the synthesis of α-HgS NEs. The NEs was precipitated by the addition of acetone. The precipitate was redispersed in a minimum volume of water and then precipitated using acetone. This procedure was repeated at three times to remove unreacted species.

Synthesis of α-HgS NTs.[46] Initially, a 100 mM thioacetamide stock solution was prepared by dissolving 60 mg of thioacetamide in 8.0 ml of water. A mercury stock solution was prepared by

dispersing 41.3 mg of $Hg(NO_3)_2 \cdot nH_2O$ in 4.0 ml of water. Then, 1.1 ml of D- or L-Pen solution (100 mM) and 0.3 ml of NaOH (1 M) were added in a sequential fashion. In a three-neck round bottom flask, 0.25 ml of D- or L-NEs colloidal solution was diluted with 2.25 ml of water under N_2 atmosphere. Then, 0.3 ml of NaOH solution (1.0 M) was added, and 0.9 ml of D- or L-Pen solution (100 mM) were added to the (+)- or (−)-NEs solution respectively. The 1.1 ml of thioacetamide stock solution and 4.0 ml of mercury stock solution containing D- or L-Pen were co-injected into the (+)- or (−)-NEs solution, respectively, for 2 h at room temperature. The reaction solution was stirred overnight and mixed with acetone, followed by centrifugation at 5000 rpm for 5 min. The precipitate was redispersed in a minimum volume of water and then precipitated using acetone. This procedure was repeated at three times to remove unreacted species.

Ligand exchange from water-soluble Pen ligands to the mixture of 1 and OAm.[49,50] In a 2-ml glass vial, 0.3 ml of an aqueous solution of α-HgS NTs or NEs was mixed with 1.5 mg of **1** in 0.05 ml of toluene and 0.05 ml of OAm. The mixture was stirred vigorously for 2 h at room temperature. After the reaction, the two phases appeared by adding 0.3 ml of water and toluene. The organic phase was carefully collected and mixed with methanol, followed by centrifugation at 5000 rpm for 5 min. The precipitate was re-dispersed in a drop of N,N-dimethylformamide (DMF) followed by re-precipitation with methanol. The washing step was repeated several times.

RESULTS AND DISCUSSION

Benzo[b]phosphole P-oxide derivatives bearing arylamine substituents exhibit excellent fluorescent properties based on the combination of a push-pull system with aggregation-induced

emission behavior.[51–54] Here, we introduced a phosphinic acid group on the benzo[b]phosphole scaffold, giving a 1-hydroxy-1H-phosphindole 1-oxide moiety (Figure 1), with the aim to anchor the molecule on the surface of α-HgS NPs.[55-57] Such binding unit was recently shown to efficiently graft on ZnO NPs leading to highly emissive hybrid NPs.[58] The anchoring phosphinic acid group was introduced as a part of the hydroxyoxophosphole moiety to have a direct interaction between the crystallographically chiral HgS surface and the fluorophore. Furthermore, the π-conjugation is extended to two bulky triarylamine groups with single bonds at the 2- and 3-positions of benzo[b]phosphole-based ring, enabling the adoption of chiral conformations with axial chirality (Figure S4). The enantiomeric interaction on the surface of intrinsically chiral HgS surface might induce such the conformational chirality. Compound **1** was synthesized in two steps from 4,4'-(ethyne-1,2-diyl)bis(N,N-bis(4-methoxyphenyl)aniline) by Ag-mediated cyclization with ethyl phenylphosphinate followed by the hydrolysis of ethyl group (see the Supporting Information for details). Photophysical study of **1** was performed in DMF (Figure S5). The absorption spectrum showed an onset of the absorption band at 450 nm with a maximum centered at 375 nm. The solution exhibits bright yellow-green emission (λ_{max} = 511 nm) with a noticeable absolute fluorescence quantum yield (Φ_F) of 0.17 under excitation at 370 nm.

HgS nanoparticles with an achiral ellipsoidal shape (NEs) were synthesized by a colloidal precipitation method using D- and L-Penicillamine (Pen). The absorption spectra gave an absorbance band at 470 nm (Figure S6), assigned to the formation of cinnabar phase.[44-46] The α-HgS NEs capped with D- and L-Pen showed positive and negative CD signals for the first Cotton effect (hereafter referred to as (+)-NEs and (–)-NEs), respectively, at 540 nm, suggesting the successful induction of crystallographic handedness depending on the chirality of Pen ligand

(Figure S6). Transmission electron microscopy (TEM) images of the both NEs exhibited an achiral shape with the same size distributions with the average width and length of 7.4 and 11.3 nm, respectively (Figure S7).[41,46,49]

With the aim of transferring the crystallographic chirality of HgS to the chiral arrangement of the achiral dye **1**, the HgS NEs were subjected to ligand exchange with **1**. We also employed oleylamine (OAm) as a co-ligand to support the dispersibility of NPs after the ligand exchange (see the Supporting Information for details).[50,59] The mixture solution of OAm and **1** in toluene was added to the aqueous dispersion of NEs to form a biphasic system, which was stirred vigorously for 2h at room temperature. The successful phase transfer of NEs from the aqueous to toluene phase was recognized by the disappearance of orange color in the former phase. Methanol, a good solvent both for OAm and **1**, was added to the organic phase to remove unbound ones followed by centrifugation, giving orange precipitate with a yellow supernatant. The precipitate could be redispersed in DMF. The increase in the absorbance below 450 nm corresponding to the light absorption by dye **1** indicates the successful anchoring of **1** on the NEs (Figure 2a). Although the HgS NEs are not a fluorescent substance, excitation to the DMF solution at 370 nm afforded an emission spectrum of which excitation spectrum was similar to the absorption spectrum of **1** (Figure S5 and Figure 2b). The less effective quenching of the emission of **1** may be ascribed to the small overlap between the emission band of **1** and the absorption edge of HgS NEs. The emission band of **1** after anchoring on NEs appeared at 525 nm, which is apparently at longer wavelength compared to that of free **1** in the same solvent (511 nm). This red-shift suggested the possible interactions between the neighboring ligands including **1** and OAm on the identical NE. Similar absorption, emission and excitation spectra were also obtained for (–)-NE@**1** (Figure S8). The size and shape of NEs were maintained as confirmed by

TEM measurement (Figure S7). While both the (+/–)-NEs@**1** were supposed to possess the similar composition to each other, they exhibited the mirror image CD spectra (Figure S9) suggesting the preservation of crystallographic chirality even after the ligand exchange with the achiral ligands of OAm and **1**.[49,50] The CD spectral shape was almost identical to that of before the ligand exchange in water (Figures S6 and S9) and no chiroptical activity assignable to **1** seemed to be superimposed in the CD spectra of NEs@**1**. Furthermore, neither of NEs@**1** afforded distinguishable CPL signal (Figure S10). While the formation of chiral conformation on the surface of intrinsically chiral HgS NPs was expected, the single point interaction through the phosphinic acid moiety is not enough to transfer chirality to the conformation of **1** (Figure S4). The ligand exchange experiment on the achiral shape HgS NEs thus resulted in the unsuccessful chirality transfer to the achiral fluorophore **1**.

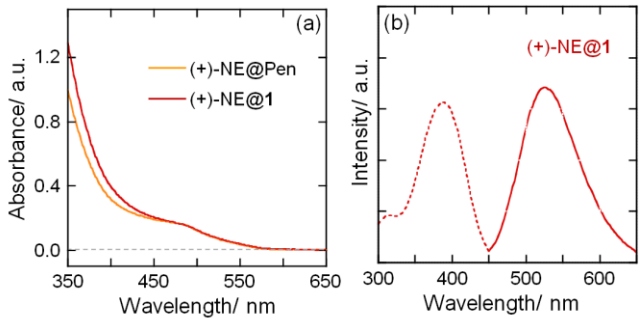

Figure 2. (a) Absorption spectra of HgS NEs capped with D-Pen ligand in water and the mixture of **1** and OAm in DMF. (b) Emission (solid line) and excitation (dotted line) spectra of HgS NEs capped with the mixture of **1** and OAm in DMF. λ_{ex} = 370 nm, λ_{em} = 525 nm.

We then explored the chirality induction to **1** on α-HgS NPs with topological chirality. α-HgS NPs with a twisted triangular bipyramid morphology (HgS NTs) were employed as a

platform of chirality transfer. α-HgS NTs were grown according to a reported procedure using (+)- and (–)-NEs as seed NPs in the presence of D- and L-Pen, respectively, controlling the handedness of twist in morphology.[46,47] Figure 3 shows typical TEM images of the epitaxially grown NTs from (+)- and (–)-NEs, possessing right-(Plus, P) and left-(Minus, M) handedness, respectively, in their twisted morphology ((+)P-NTs and (−)M-NTs, respectively). The average length and aspect ratio of NTs are in the ranges of 90-100 nm and 1.75-1.90, respectively, similar to the previous report,[46] corresponding to the helical twisting angle of ca. 60º in the twisted morphology of the NTs. Since the size of NPs increased to almost 100 nm, the non-negligible effect of light scattering appeared in the absorption spectra (Figure S11). While no apparent difference was found in the absorption profile between (+)P- and (−)M-NTs, the NTs displayed mirror-image CD spectra in the visible region, supporting the preservation of crystallographic chirality (Figure 4). The chiral twisted topology modified the CD profile around 450 and over 500 nm to a certain degree (Figure S6 and Figure 4).

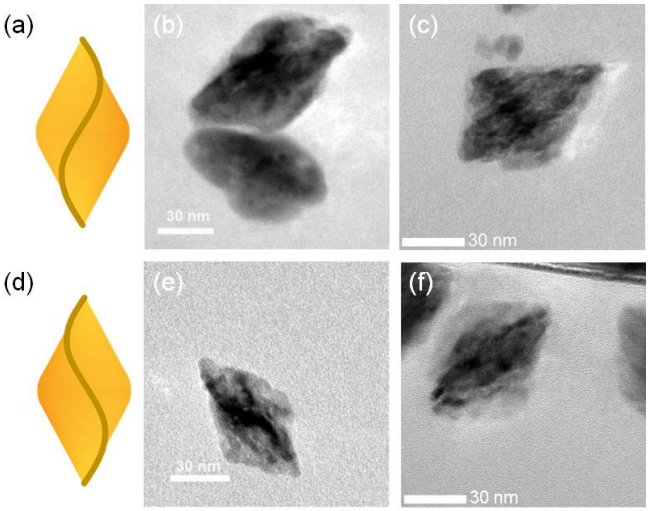

Figure 3. Schematic models (a) (+)P-NT and (d) (–)M-NT together with TEM images (b) (+)P-NT@D-Pen, (c) (+)P-NT@**1**, (e) (–)M-NT@L-Pen and (f) (–)M-NT@**1**.

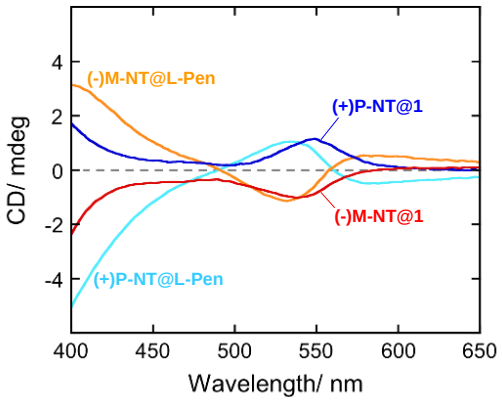

Figure 4. CD spectra of (+)P-NT@D-Pen (cyan), (–)M-NT@L-Pen (orange), (+)P-NT@**1** (blue), and (–)M-NT@**1** (red).

In a similar manner to the HgS NEs, the HgS NTs were also subjected to ligand exchange with the mixture of OAm and **1**.[49] The NTs were purified by repetitive dispersion/reprecipitation cycles to remove unbound ligands. After the ligand exchange process, the NTs (NT@**1**) were also dispersed in DMF. The ligand exchange was evaluated with attenuated total reflection Fourier transform infrared (ATR-FTIR) study (Figure S12). A small band around 1000 cm^{-1} corresponding to ν(P-OH)[58] in the free ligand was observed to disappear on (+)P-NTs, as a proof of the grafting. The phosphoric (P(=O)OH) group of free **1** gave characteristic peaks at 1267 and 1059 cm^{-1} corresponding to stretching modes of phosphine oxide ν(P=O) and phosphinate ν(POO^-), respectively.[60,61] The latter peak broadened and shifted to a lower wavenumber in (+)P-NT@**1**, indicating that the POO^- group coordinates to the NT-surface. Furthermore, the

disappearance of the ν(P=O) peak around 1260 cm^{-1} suggests the bridging or chelating coordination mode, where the POO^- group interacts with the surface using both oxygen atoms.

The ligand-exchange procedure had little effect on the size and shape of NTs (Figure 3). TEM images of (+)P- and (–)M-NT@**1** demonstrated no obvious change in the size and shape of the NTs, confirming that the chiral morphology remained unchanged after the ligand exchange. The NT@**1** preserved the optical activity with an identical sign of the Cotton effect over 450 nm to the corresponding NTs before the ligand exchange, thus demonstrating the preservation of the crystallographic chirality in the NT core (Figure 4).

The successful modification of NTs with **1** was further supported by UV-vis absorption and emission spectra (Figure 5). The ligand-exchanged NTs gave an increase in the absorbance below 450 nm compared to the Pen-capped NTs. Both the (+)P- and (–)M-NT@**1** exhibited yellow-green emission with maxima at around 520–530 nm (Figure 5b), respectively, which red-shifted compared to that of free **1** in a similar manner to the NEs@**1**. The excitation spectra of the NT@**1** monitored at 525 nm were identical with that of free **1** (Figure S13), indicating that the observed emission stems from capped **1** and that excitonic energy transfer from the HgS NT core did not take place. The amount of **1** on the NT-surface was reduced by decreasing the charging amount of **1** in the ligand-exchange procedure. The decrease in the amount of surface-bound **1** resulted in the decrease of emission intensity as well as a prominent blue-shift of emission spectrum (Figure S14), indicating the decreased intermolecular interaction of **1** with decreasing the grafting density on the surface of NTs.

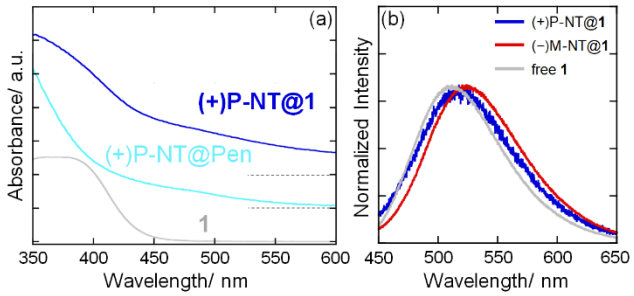

Figure 5. (a) Absorption spectra of **1** and (+)P-NT@**1** in DMF and (+)P-NT@Pen in water. (b) Emission spectra of **1**, (+)P-NT@**1** and (–)M-NT@**1** in DMF.

Interestingly, the (+)P- and (–)M-NT@**1** exhibited intense CPL signals around fluorescence maxima, while no CPL signal was detected for free **1** (Figure 6). Although the spectral shapes were not very clear mirror images to each other, the distinct positive and negative CPL signals were recorded for the (+)P- and (–)M-NT@**1**, respectively. The intensity of CPL can be evaluated by the luminescence dissymmetry factor (g_{lum}), which is defined as $g_{lum} = 2(I_L - I_R)/(I_L + I_R)$, where I_L and I_R are the intensities of left- and right-handed circularly polarized emission, respectively. The $|g_{lum}|$ values at the peak wavelength were about 0.004 for both NT@**1**. Since the achiral shaped NEs could not induce the CPL activity to the achiral dye **1**, the topological chirality of NTs should play a role in this chirality induction.

The role of chiral morphology of HgS NTs in the chirality induction of **1** could be figured out by employing HgS NTs with different handedness combinations of crystalline lattice and morphology. The twisting direction of HgS NTs could be controlled independently from the crystallographic chirality of HgS, enabling the synthesis of (+)M- and (–)P-NTs by using a combination of opposite enantiomeric Pen-ligands in the seed preparation and growth stages.[46] The (+)-NEs prepared with D-Pen were used as a seed for the growth of M-NTs in the presence

of L-Pen for the synthesis of (+)M-NTs, and vice versa for (–)P-NTs. Each NTs exhibited a CD profile with the sign of Cotton effect over 500 nm identical to the original seed NEs (Figure S15), indicating the preserved crystallographic handedness of HgS seed after the epitaxial growth. TEM images of the NTs revealed that M- and P-twisted morphologies were grown on the (+)- and (–)-NE seeds with a similar average length of 50 nm (Figure S16). The ligand exchange procedure with the mixture of OAm/**1** afforded (+)M- and (–)P-NTs@**1** dispersed in DMF with spectroscopic characteristics similar to those of (+)P- and (–)M-NT@**1** (Figures S17, 18), suggesting the successful preparation of **1**-modified (+)M- and (–)P-NTs. The CD spectral profiles over 450 nm are mostly preserved for (+)M- and (–)P-NT@**1** after the ligand exchange, indicating that the ligand exchange did not have an effect on the crystallographic chirality of the NTs (Figure S15). As shown in Figure 6, the NTs@**1** displayed CPL signals with amplitudes comparable to those of NTs with other chirality combinations ($|g_{lum}| \sim 0.004$). A negative CPL signal was observed for the (+)M-NT@**1**, whereas a positive one was recorded for the (−)P-NT@**1**. Considering this result together with that of (+)P- and (−)M-NTs@**1**, it should be noted that the sign of CPL signal is regulated not by the crystallographic chirality but the morphological chirality of the twisted bipyramid NTs. The importance of topological chirality in the chirality induction was further confirmed by employing NPs with an achiral rod shape (NRs, Figures S19–S21). Although the NRs@**1** exhibited a fluorescence spectrum ascribed to **1**, they afforded no identifiable CPL activity in a similar manner to the NEs with a smaller size (Figure S10).

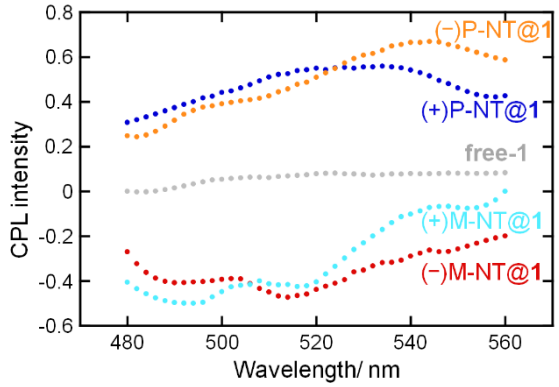

Figure 6. CPL spectra of free **1**, (+)P-NT@**1**, (+)P-NT@**1**, (–)M-NT@**1** and (+)M-NT@**1**.

The typical radius of surface curvature of the NTs is about 30-50 nm, which seems too large to have an impact on the unimolecular conformation of individual **1** for inducing the conformational chirality. Given the monodentate nature of the achiral dye **1** in anchoring on the surface of NPs, it seems difficult to induce a chiral twist to the conformational geometry in **1** adsorbed on NPs. The crystallographic chirality thus could not serve as a source of chirality induction from inorganic NPs to achiral dye **1** as demonstrated by the absence of induced CPL in the NEs@**1** and NR@**1**. One may also consider the selective quenching of right or left circularly polarized light by the optically active chiral HgS NPs. However, the effect of optical activity of NPs could be excluded by considering the correlation of sings between the CD and CPL signals. For example, both (+)P- and (+)M-NTs@**1** afforded the positive first Cotton effect around 530 nm stemming from the crystallographic chirality of cinnabar phase, whereas the former and latter NPs exhibited a positive and negative CPL signal, respectively.

The chirality is, therefore, considered to be induced in the arrangement, or assembly of compound **1** on the helically curved surface (Figure 7). The red-shift in the emission spectrum

with increasing the grafting density of **1** (Figure S14) also supports the intermolecular interaction of **1** on the surface of NTs. Regardless of the lattice handedness, right-handed arrangement of **1** could be attained on the NPs with a right-handed twist (P-NTs), generating positive CPL, and vice versa on the M-NTs (Figure 6). Recently, Fernández-Lázaro, Bassani, Oda and coworkers reported the chirality induction to achiral dye molecules on the nanometric silica helices.[41] The surface of helical silica with topological chirality (helical pitch ~65 nm and diameter ~35 nm) was modified with achiral chromophores via a single-point covalent interaction. The chiral positive curvature of helical silica surface was expected to give a slight offset in the arrangement of anchored chromophores, imparting a relative rotation in the direction vectors of their electronic transition dipole moments.[41,62] While the chiral curvature was negative on the NTs surface, the similar effect is expected to operate on the surface-bound **1**. The exciton coupling mechanism, which works on the helically arranged vicinal chromophores,[61] is responsible for the emergence of induced CD[41] or CPL. The chiral induction on the surface of silica helices was successfully evaluated by the induced CD of achiral dyes.[41] As a preliminary test, we also tried to extract the optical activity derived from the chiral interaction between **1** with substruction of the CD profile assigned to NT@OAm from that of NT@**1** as a back ground signal (Figure S22). Although the differential CD spectra were not mirror images to each other, the (+)P- and (-)M-NTs afforded a positive and negative Cotton effect, respectively, in the absorption region of achiral dye **1** (370–440 nm). The CD sing accorded with that of corresponding CPL signal, supporting the induction of chirality in the assembly of **1** on the NT surface.

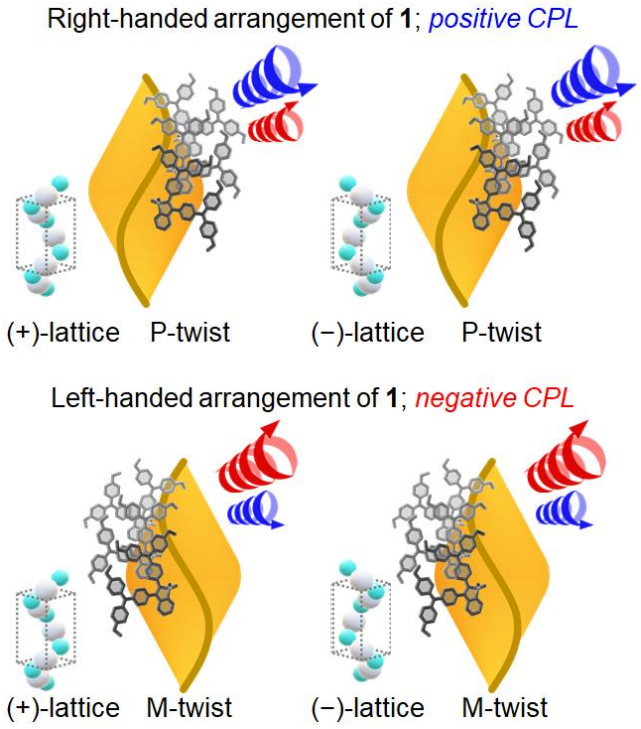

Figure 7. Schematic illustration of the induced CPL generation on the chirally shaped HgS NTs.

CONCLUSION

In conclusion, we have developed a new approach to generate hybrid CPL-active materials composed of a chiral inorganic nanoparticle and achiral fluorescent ligands incorporating a grafting unit. The achiral molecule **1** adsorbed on the helically twisted surface of α-HgS NTs exhibited noticeable CPL signals depending on the morphological chirality of NTs, regardless of the crystallographic chirality. The chiral negative curvature on the surface of NTs was considered to serve a platform for the chiral assembly of achiral dye **1**, giving rise to induced CPL. The α-HgS NTs could possess both handedness in the crystalline lattice and nanoparticle morphology. The present work demonstrated the latter played a key role in the chirality transfer from the curved surface of NTs to the arrangement of achiral **1**. Further design of organic

luminescent molecules with appropriate coordinating groups would demonstrate the utility of the present chiral-inorganic and organic hybrid system as versatile CPL generation systems.

ASSOCIATED CONTENT

Supporting Information.

The Supporting Information is available free of charge at https://pubs.acs.org/doi/10.1021/ Detailed synthetic procedures and chemical identifications of compound **1**, supplemental spectroscopic data and TEM images (PDF).

AUTHOR INFORMATION

Corresponding Authors

*Takuya Nakashima, Department of Chemistry, Graduate School of Science, Osaka Metropolitan University, Osaka 558-8585, Japan, E-mail: takuya.nakashima@omu.ac.jp

*Tsuyoshi Kawai, Division of Materials Science, Graduate School of Science and Technology, Nara Institute of Science and Technology, Nara 630-0192, Japan, E-mail: tkawai@ms.naist.jp

*Muriel Hissler, Univ Rennes, CNRS, ISCR - UMR 6226, F-35000 Rennes, France, E-mail: muriel.hissler@univ-rennes1.fr

Notes

The authors declare no competing financial interest.

ACKNOWLEDGMENT

This work was supported by JSPS KAKENHI grant numbers JP16H06522 in Scientific Research on Innovative Areas “Coordination Asymmetry”, JP22H05134 for Transformative Research

Areas (A) “Revolution of Chiral Materials Science using Helical Light Fields”, and the Ministère de la Recherche et de l’Enseignement Supérieur, the CNRS, the Région Bretagne, the French National Research Agency (ANR Fluohyb ANR-17-CE09-0020). J. K. acknowledges a JSPS Research Fellowship for Young Scientists.

REFERENCES

1. Schadt, M. Liquid Crystal Materials and Liquid Crystal Displays. *Annu. Rev. Mater. Sci.* **1997,** *27*, 305-379.
2. Zinna, F.; Giovanella, U.; Di Bari, L. Highly Circularly Polarized Electroluminescence from a Chiral Europium Complex. *Adv. Mater.* **2015,** *27*, 1791-1795.
3. Kim, Y.; Yeom, B.; Arteaga, O.; Jo Yoo, S.; Lee, S. G.; Kim, J. G.; Kotov, N. A. Reconfigurable Chiroptical Nanocomposites with Chirality Transfer from the Macro- to the Nanoscale. *Nat. Mater.* **2016,** *15*, 461-468.
4. Imai, Y.; Nakano, Y.; Kawai, T.; Yuasa, J. A Smart Sensing Method for Object Identification Using Circularly Polarized Luminescence from Coordination-Driven Self-Assembly. *Angew. Chem. Int. Ed.* **2018,** *57*, 8973-8978.
5. Yang, Y.; da Costa, R. C.; Fuchter, M. J.; Campbell, A. J. Circularly Polarized Light Detection by a Chiral Organic Semiconductor Transistor. *Nat. Photon.* **2013,** *7*, 634-638.
6. Imagawa, T.; Hirata, S.; Totani, K.; Watanabe, T.; Vacha, M. Thermally Activated Delayed Fluorescence with Circularly Polarized Luminescence Characteristics. *Chem. Commun.* **2015,** *51*, 13268-13271.
7. Feuillastre, S.; Pauton, M.; Gao, L.; Desmarchelier, A.; Riives, A. J.; Prim, D.; Tondelier, D.; Geffroy, B.; Muller, G.; Clavier, G.; Pieters. G. Design and Synthesis of New Circularly Polarized Thermally Activated Delayed Fluorescence Emitters. *J. Am. Chem. Soc.* **2016,** *138*, 3990-3993.
8. Frederic, L.; Desmarchelier, A.; Plais, R.; Lavnevich, L.; Muller, G.; Villafuerte, C.; Clavier, G.; Quesnel, E.; Racine, B.; Meunier-Della-Gatta, S.; Dognon, J. P.; Thuery, P.; Crassous, J.; Favereau, L.; Pieters, G.. Maximizing Chiral Perturbation on Thermally Activated Delayed

Fluorescence Emitters and Elaboration of the First Top-Emission Circularly Polarized Oled. *Adv. Funct. Mater.* **2020,** *30*, 2004838.

9. Chen, C.; Gao, L.; Gao, W.; Ge, C.; Du, X.; Li, Z.; Yang, Y.; Niu, G.; Tang, J., Circularly Polarized Light Detection Using Chiral Hybrid Perovskite. *Nat. Commun.* **2019,** *10*, 1927.
10. Sharma, N.; Spuling, E.; Mattern, C. M.; Li, W.; Fuhr, O.; Tsuchiya, Y.; Adachi, C.; Brase, S.; Samuel, I. D. W.; Zysman-Colman, E., Turn on of Sky-Blue Thermally Activated Delayed Fluorescence and Circularly Polarized Luminescence (CPL) Via Increased Torsion by a Bulky Carbazolophane Donor. *Chem. Sci.* **2019,** *10*, 6689-6696.
11. Sanchez-Carnerero, E. M.; Agarrabeitia, A. R.; Moreno, F.; Maroto, B. L.; Muller, G.; Ortiz, M. J.; de la Moya, S. Circularly Polarized Luminescence from Simple Organic Molecules. *Chem. Eur. J.* **2015,** *21*, 13488-13500.
12. Brandt, J. R.; Salerno, F.; Fuchter, M. J. The Added Value of Small-Molecule Chirality in Technological Applications. *Nat. Rev. Chem.* **2017,** *1*, 0045.
13. Chen, N.; Yan, B. Recent Theoretical and Experimental Progress in Circularly Polarized Luminescence of Small Organic Molecules. *Molecules* **2018,** *23*, 3376.
14. Tanaka, H.; Inoue, Y.; Mori, T. Circularly Polarized Luminescence and Circular Dichroisms in Small Organic Molecules: Correlation between Excitation and Emission Dissymmetry Factors. *ChemPhotoChem* **2018,** *2*, 386-402.
15. Langeveld-Voss, B. M. W.; Janssen, R. A. J.; Christiaans, M. P. T.; Meskers, S. C. J.; Dekkers, H. P. J. M.; Meijer, E. W. Circular Dichroism and Circular Polarization of Photoluminescence of Highly Ordered Poly{3,4-Di[(*S*)-2-Methylbutoxy]Thiophene}. *J. Am. Chem. Soc.* **1996,** *118*, 4908-4909.
16. Peeters, E.; Christiaans, M. P. T.; Janssen, R. A. J.; Schoo, H. F. M.; Dekkers, H. P. J. M.; Meijer, E. W. Circularly Polarized Electroluminescence from a Polymer Light-Emitting Diode. *J. Am. Chem. Soc.* **1997,** *119*, 9909-9910.
17. Shiraki, T.; Tsuchiya, Y.; Noguchi, T.; Tamaru, S.; Suzuki, N.; Taguchi, M.; Fujiki, M.; Shinkai, S. Creation of Circularly Polarized Luminescence from an Achiral Polyfluorene Derivative through Complexation with Helix-Forming Polysaccharides: Importance of the Meta-Linkage Chain for Helix Formation. *Chem. Asian J.* **2014,** *9*, 218-222.

18. Albano, G.; Pescitelli, G.; Di Bari, L. Chiroptical Properties in Thin Films of Pi-Conjugated Systems. *Chem. Rev.* **2020,** *120*, 10145-10243.

19. Zinna, F.; Di Bari, L. Lanthanide Circularly Polarized Luminescence: Bases and Applications. *Chirality* **2015,** *27*, 1-13.

20. Kitagawa, Y.; Tsurui, M.; Hasegawa, Y. Steric and Electronic Control of Chiral Eu(Iii) Complexes for Effective Circularly Polarized Luminescence. *ACS Omega* **2020,** *5*, 3786-3791.

21. Gauthier, E. S.; Abella, L.; Hellou, N.; Darquie, B.; Caytan, E.; Roisnel, T.; Vanthuyne, N.; Favereau, L.; Srebro-Hooper, M.; Williams, J. A. G.; Autschbach, J.; Crassous, J. Long-Lived Circularly Polarized Phosphorescence in Helicene-Nhc Rhenium(I) Complexes: The Influence of Helicene, Halogen, and Stereochemistry on Emission Properties. *Angew. Chem. Int. Ed.* **2020,** *59*, 8394-8400.

22. Tan, Y. B.; Okayasu, Y.; Katao, S.; Nishikawa, Y.; Asanoma, F.; Yamada, M.; Yuasa, J.; Kawai, T. Visible Circularly Polarized Luminescence of Octanuclear Circular Eu(Iii) Helicate. *J. Am. Chem. Soc.* **2020,** *142*, 17653-17661.

23. Kumar, J.; Nakashima, T.; Kawai, T. Circularly Polarized Luminescence in Chiral Molecules and Supramolecular Assemblies. *J. Phys. Chem. Lett.* **2015,** *6*, 3445-3452.

24. Sang, Y.; Han, J.; Zhao, T.; Duan, P.; Liu, M. Circularly Polarized Luminescence in Nanoassemblies: Generation, Amplification, and Application. *Adv. Mater.* **2020,** *32*, e1900110.

25. Mori, T. Ed. *Circularly Polarized Luminescence of Isolated Small Organic Molecules*; Springer: Singapore, 2020.

26. Brittain, H. G. Excited-State Optical Activity of a Cyclodextrin Inclusion Compound. *Chem. Phys. Lett.* **1981,** *83,* 161-164.

27. Flamigni, L. Inclusion of Fluorescein and Halogenated Derivatives In α-, β-, and γ-Cyclodextrins: A Steady-State and Picosecond Time-Resolved Study. *J. Phys. Chem.* **2002,** *97,* 9566-9572.

28. Haraguchi, S.; Numata, M.; Li, C.; Nakano, Y.; Fujiki, M.; Shinkai, S. Circularly Polarized Luminescence from Supramolecular Chiral Complexes of Achiral Conjugated Polymers and a Neutral Polysaccharide. *Chem. Lett.* **2009,** *38*, 254-255.

29. Goto, T.; Okazaki, Y.; Ueki, M.; Kuwahara, Y.; Takafuji, M.; Oda, R.; Ihara, H. Induction of Strong and Tunable Circularly Polarized Luminescence of Nonchiral, Nonmetal, Low-Molecular-Weight Fluorophores Using Chiral Nanotemplates. *Angew. Chem. Int. Ed.* **2017,** *56*, 2989-2993.

30. Han, J.; You, J.; Li, X.; Duan, P.; Liu, M. Full-Color Tunable Circularly Polarized Luminescent Nanoassemblies of Achiral Aiegens in Confined Chiral Nanotubes. *Adv. Mater.* **2017,** *29*, 1606503.

31. Zhang, J.; Liu, Q.; Wu, W.; Peng, J.; Zhang, H.; Song, F.; He, B.; Wang, X.; Sung, H. H.; Chen, M.; Li, B. S.; Liu, S. H.; Lam, J. W. Y.; Tang, B. Z. Real-Time Monitoring of Hierarchical Self-Assembly and Induction of Circularly Polarized Luminescence from Achiral Luminogens. *ACS Nano* **2019,** *13*, 3618-3628.

32. Huo, S.; Duan, P.; Jiao, T.; Peng, Q.; Liu, M. Self-Assembled Luminescent Quantum Dots to Generate Full-Color and White Circularly Polarized Light. *Angew. Chem. Int. Ed.* **2017,** *56*, 12174-12178.

33. Jin, X.; Sang, Y.; Shi, Y.; Li, Y.; Zhu, X.; Duan, P.; Liu, M. Optically Active Upconverting Nanoparticles with Induced Circularly Polarized Luminescence and Enantioselectively Triggered Photopolymerization. *ACS Nano* **2019,** *13*, 2804-2811.

34. Shi, Y.; Duan, P.; Huo, S.; Li, Y.; Liu, M. Endowing Perovskite Nanocrystals with Circularly Polarized Luminescence. *Adv. Mater.* **2018,** *30*, e1705011.

35. Wang, Y.-J.; Jin, Y.; Shi, X.-Y.; Dong, X.-Y.; Zang, S.-Q. Achiral Copper Clusters Helically Confined in Self-Assembled Chiral Nanotubes Emitting Circularly Polarized Phosphorescence. *Inorg. Chem. Front.* **2022,** *9*, 3330-3334.

36. Sugimoto, M.; Liu, X. L.; Tsunega, S.; Nakajima, E.; Abe, S.; Nakashima, T.; Kawai, T.; Jin, R. H. Circularly Polarized Luminescence from Inorganic Materials: Encapsulating Guest Lanthanide Oxides in Chiral Silica Hosts. *Chem. Eur. J.* **2018,** *24*, 6519-6524.

37. Tsunega, S.; Jin, R. H.; Nakashima, T.; Kawai, T. Transfer of Chiral Information from Silica Hosts to Achiral Luminescent Guests: A Simple Approach to Accessing Circularly Polarized Luminescent Systems. *ChemPlusChem* **2020,** *85,* 619-626.

38. Liu, P.; Chen, W.; Okazaki, Y.; Battie, Y.; Brocard, L.; Decossas, M.; Pouget, E.; Muller-Buschbaum, P.; Kauffmann, B.; Pathan, S.; Sagawa, T.; Oda, R. Optically Active Perovskite $CsPbBr_3$ Nanocrystals Helically Arranged on Inorganic Silica Nanohelices. *Nano Lett.* **2020,** *20*, 8453-8460.

39. Dolamic, I.; Varnholt, B.; Burgi, T. Chirality Transfer from Gold Nanocluster to Adsorbate Evidenced by Vibrational Circular Dichroism. *Nat. Commun.* **2015,** *6*, 7117.

40. Wei, X.; Liu, J.; Xia, G. J.; Deng, J.; Sun, P.; Chruma, J. J.; Wu, W.; Yang, C.; Wang, Y. G.; Huang, Z. Enantioselective Photoinduced Cyclodimerization of a Prochiral Anthracene Derivative Adsorbed on Helical Metal Nanostructures. *Nat. Chem.* **2020,** *12*, 551-559.

41. Scalabre, A.; Gutiérrez-Vílchez, A. M.; Sastre-Santos, Á.; Fernández-Lázaro, F.; Bassani, D. M.; Oda, R. Supramolecular Induction of Topological Chirality from Nanoscale Helical Silica Scaffolds to Achiral Molecular Chromophores. *J. Phys. Chem. C* **2020,** *124*, 23839-23843.

42. Harada, T.; Yanagita, H.; Ryu, N.; Okazaki, Y.; Kuwahara, Y.; Takafuji, M.; Nagaoka, S.; Ihara, H.; Oda, R. Lanthanide Ion-Doped Silica Nanohelix: A Helical Inorganic Network Acts as a Chiral Source for Metal Ions. *Chem. Commun.* **2021,** *57*, 4392-4395.

43. Chen, J.; Gao, X.; Zheng, Q.; Liu, J.; Meng, D.; Li, H.; Cai, R.; Fan, H.; Ji, Y.; Wu, X. Bottom-up Synthesis of Helical Plasmonic Nanorods and Their Application in Generating Circularly Polarized Luminescence. *ACS Nano* **2021**, *15*, 15114-15122.

44. Ben-Moshe, A.; Govorov, A. O.; Markovich, G. Enantioselective Synthesis of Intrinsically Chiral Mercury Sulfide Nanocrystals. *Angew. Chem. Int. Ed.* **2013,** *52*, 1275-1279.

45. Kuno, J.; Miyake, K.; Katao, S.; Kawai, T.; Nakashima, T. Enhanced Enantioselectivity in the Synthesis of Mercury Sulfide Nanoparticles through Ostwald Ripening. *Chem. Mater.* **2020,** *32*, 8412-8419.

46. Wang, P. P.; Yu, S. J.; Govorov, A. O.; Ouyang, M. Cooperative Expression of Atomic Chirality in Inorganic Nanostructures. *Nat. Commun.* **2017,** *8*, 14312.

47. Cao, Z.; He, J.; Liu, Z.; Zhang, H.; Chen, B. Chirality Affecting Reaction Dynamics of HgS Nanostructures Simultaneously Visualized in Real and Reciprocal Space. *ACS Nano* **2021,** *15*, 16255-16265.

48. Tsumatori, H.; Nakahsima, T.; Kawai, T. Observation of Chiral Aggregate Growth of Perylene Derivative in Opaque Solution by Circularly Polarized Luminescence. *Org. Lett.* **2010**, *10*, 2362-2365.

49. Wang, P. P.; Yu, S. J.; Ouyang, M. Assembled Suprastructures of Inorganic Chiral Nanocrystals and Hierarchical Chirality. *J. Am. Chem. Soc.* **2017,** *139*, 6070-6073.

50. Kuno, J.; Kawai, T.; Nakashima, T. The Effect of Surface Ligands on the Optical Activity of Mercury Sulfide Nanoparticles. *Nanoscale* **2017,** *9*, 11590-11595.

51. Yamaguchi, E.; Fukazawa, A.; Kosaka, Y.; Yokogawa, D.; Irle, S.; Yamaguchi, S. A Benzophosphole P-Oxide with an Electron-Donating Group at 3-Position: Enhanced Fluorescence in Polar Solvents. *Bull. Chem. Soc. Jpn.* **2015,** *88*, 1545-1552.

52. Wang, C.; Fukazawa, A.; Taki, M.; Sato, Y.; Higashiyama, T.; Yamaguchi, S. A Phosphole Oxide Based Fluorescent Dye with Exceptional Resistance to Photobleaching: A Practical Tool for Continuous Imaging in Sted Microscopy. *Angew. Chem. Int. Ed.* **2015,** *54*, 15213-15217.

53. Matano, Y.; Motegi, Y.; Kawatsu, S.; Kimura, Y. Comparison of 2-Arylnaphtho[2,3-b]Phospholes and 2-Arylbenzo[b]Phospholes: Effects of 2-Aryl Groups and Fused Arene Moieties on Their Optical and Photophysical Properties. *J. Org. Chem.* **2015,** *80*, 5944-5950.

54. Zhuang, Z.; Bu, F.; Luo, W.; Peng, H.; Chen, S.; Hu, R.; Qin, A.; Zhao, Z.; Tang, B. Z. Steric, Conjugation and Electronic Impacts on the Photoluminescence and Electroluminescence Properties of Luminogens Based on Phosphindole Oxide. *J. Mater. Chem. C* **2017,** *5*, 1836-1842.

55. Puzder, A.; Williamson, A. J.; Zaitseva, N.; Galli, G.; Manna, L.; Alivisatos, A. P. The Effect of Organic Ligand Binding on the Growth of Cdse Nanoparticles Probed by Ab Initio Calculations. *Nano Lett.* **2004,** *4*, 2361-2365.

56. Owen, J. S.; Park, J.; Trudeau, P. E.; Alivisatos, A. P. Reaction Chemistry and Ligand Exchange at Cadmium-Selenide Nanocrystal Surfaces. *J. Am. Chem. Soc.* **2008,** *130,* 12279-12281.

57. Hassinen, A.; Gomes, R.; De Nolf, K.; Zhao, Q.; Vantomme, A.; Martins, J. C.; Hens, Z. Surface Chemistry of CdTe Quantum Dots Synthesized in Mixtures of Phosphonic Acids and Amines: Formation of a Mixed Ligand Shell. *J. Phys. Chem. C* **2013,** *117,* 13936-13943.

58. Phelipot, J.; Ledos, N.; Dombray, T.; Duffy, M. P.; Denis, M.; Wang, T.; Didane, Y.; Gaceur, M.; Bao, Q.; Liu, X.; Fahlman, M.; Delugas, P.; Mattoni, A.; Tondelier, D.; Geffroy, B.; Bouit, P. A.; Margeat, O.; Ackermann, J.; Hissler, M. Highly Emissive Layers Based on Organic/Inorganic Nanohybrids Using Aggregation Induced Emission Effect. *Adv. Mater. Technol.* **2021,** *7*, 2100876.

59. Chakraborty, I. N.; Roy, P.; Rao, A.; Devatha, G.; Roy, S.; Pillai, P. P. The Unvconventional Role of Surface Ligands in Dictating the Light Harvesting Properties of Quantum Dots. *J. Mater. Chem. A.* **2021**, *9*, 7422-7457.

60. Khawaja, E. E.; Durrani, S. M. A.; Al-Adel, F. F.; Salim, M. A.; Hussain, M. S. X-Ray Photoelectron Spectroscopy and Fourier Transform-Infrared Studies of Transition Metal Phosphate Glasses. *J. Mater. Sci.* **1995,** *30*, 225-234.

61. Marivel, S.; Shimpi, M. R.; Pedireddi, V. R. Novel Supramolecular Assemblies of Coordination Polymers of Zn(II) and Bis(4-Nitrophenyl)Phosphoric Acid with Some Aza-Donor Compounds. *Cryst. Growth Des.* **2007,** *7*, 1791-1796.

62. Harada, N.; Nakanishi, K. *Circular Dichroism Spectroscopy – Exciton Coupling in Organic Spectrochemistry*; Oxford University Press: Oxford, 1983.

Figure for TOC